EFFECTS OF CYCLASE-ASSOCIATED PROTEIN 2 α-ACTIN INDUCED ISOFORM EXCHANGE ON ACTOMYOSIN INTERACTIONS

by

Ryan M. Bowser

A Thesis Submitted to the Faculty of the

DEPARTMENT OF MOLECULAR AND CELLULAR BIOLOGY

In Partial Fulfillment of the Requirements

For the Degree of

MASTER OF SCIENCE

In the Graduate College

THE UNIVERSITY OF ARIZONA

2025

THE UNIVERSITY OF ARIZONA
GRADUATE COLLEGE

As members of the Master's Committee, we certify that we have read the thesis prepared by: Ryan Bowser
titled: EFFECTS OF CYCLASE-ASSOCIATED PROTEIN 2 a-ACTIN INDUCED ISOFORM EXCHANGE ON ACTOMYOSIN INTERACTIONS

and recommend that it be accepted as fulfilling the thesis requirement for the Master's Degree.

Lisa M Nagy
Lisa Nagy — Date: Apr 18, 2025

Guang Yao
Guang Yao — Date: Apr 18, 2025

Carol Gregorio
Carol Gregorio — Date: Apr 21, 2025

_____ — Date: _____

Final approval and acceptance of this thesis is contingent upon the candidate's submission of the final copies of the thesis to the Graduate College.

I hereby certify that I have read this thesis prepared under my direction and recommend that it be accepted as fulfilling the Master's requirement.

Carol Gregorio — Date: Apr 21, 2025
Carol Gregorio
Cellular & Molecular Medicine

ACKNOWLEDGEMENTS

First and foremost, I would like to acknowledge and deeply thank my mentor Dr. Gerrie P. Farman, whose impact on this thesis and my career is truly immeasurable. Without his guidance and expertise, this would not have been possible. Similarly, I would like to show my deepest appreciation for my PI and Thesis Advisor, Dr. Carol C. Gregorio, who has provided support and opportunity throughout my entire time in her laboratory. My incredible lab mates and other mentors: Tania Larrinaga, Chris Pappas, and Tim Rast have all taught me an incredible amount of knowledge, as well as being wonderful people and lab mates from the first day I joined the lab. Finally, I would like to acknowledge my parents, brother, and girlfriend for being immense sources of support throughout my life and education.

LAND ACKNOWLEDGEMENT

We respectfully acknowledge the University of Arizona is on the land and territories of Indigenous peoples. Today, Arizona is home to 22 federally recognized tribes, with Tucson being home to the O'odham and the Yaqui. Committed to diversity and inclusion, the University strives to build sustainable relationships with sovereign Native Nations and Indigenous communities through education offerings, partnerships, and community service.

TABLE OF CONTENTS

LIST OF FIGURES

ABSTRACT

Cyclase-associated protein 2 (CAP2) plays a critical role in thin filament maturation by mediating the exchange of α-actin isoforms within the sarcomere. In CAP2 knockout (CAP2-KO) mice, this process is disrupted, resulting in a significant increase in smooth muscle actin (SMA) and skeletal actin (SKA) and decreased levels of cardiac actin (CAA). Therefore, CAP2-KO disease correlates the altered isoform profile with cardiac dysfunction and the development of dilated cardiomyopathy (DCM). Using single-cell mechanics, this study shows that CAP2-KO cardiomyocytes have significantly reduced force production at maximal calcium activation, which is rescued by an overexpression of CAA. *In vitro* motility (IVM) assays demonstrate that only regulated thin filaments display functional differences in actin-myosin interactions between isoforms, likely mediated through SMA's increased binding to the troponin complex. These findings support a model in which α-actin isoform expression impacts actomyosin interactions indirectly through regulation by accessory proteins, contributing to the contractile dysfunction seen in CAP2-KO hearts.

INTRODUCTION

Cardiovascular Disease and Health

Cardiovascular disease (CVD) has solidly established itself as a healthcare epidemic in the United States and around the world. Standing as the leading cause of death in the United States, CVD results in 700,000 deaths a year and costs the U.S. economy a staggering $250 billion annually. [2] Unfortunately, these statistics are only expected to grow in the coming years, with the cost of CVD projected to exceed $1.3 trillion by 2050 [3], thus it is clear that there is an urgent need for research into prevention, mechanisms, and cures for CVD. Despite the impact of cardiovascular disease, much is still unknown about the origins of the disease and molecular mechanisms for how CVD progresses over time. It is known that there are universal behavioral risk factors that can increase an individual's risk for developing CVD (such as age, cigarette smoking, cholesterol, etc.) [4]. Still, genetic risk factors have been a rapidly developing field of research. In particular, there is a form of cardiovascular disease called dilated cardiomyopathy (DCM) with a high prevalence of cases (30% to 50%) caused by genetic defects [5].

DCM is characterized by an enlargement of the heart's left ventricle, thinning of the heart walls, and weaker contraction of cardiac tissue, leading to a decreased amount of oxygenated blood being pushed from the heart [5]. This is a debilitating disease, with five-year mortality rates of approximately 50%, and a typically autosomal dominant phenotype that can affect individuals throughout families [5, 6]. Research has shown numerous genetic mutations that can cause DCM [7], but a single central mechanism has not been demonstrated. Therefore, investigation into the many different ways this disease can occur is critically important for improving the survival outcomes of DCM patients. By investigating unique ways that this disease can occur, we gain a better understanding of the proteins important for cardiovascular function, opening the door for treatments down the road.

Muscle Contraction and Actin Isoforms

The contraction of striated muscle within the body is a critical function, from pumping oxygen-rich blood throughout the body to enabling movement and maintaining posture. Within the vasculature, contraction and relaxation of smooth muscle cells constrict and dilate blood vessels, modulating blood pressure and maintaining proper perfusion of body tissue and organs.

Underlying these crucial functions are interactions between the motor protein myosin and the structural protein actin. To enable contraction, myosin transitions through its ATPase cycle, hydrolyzing ATP, binding filamentous actin, and releasing ADP to result in a conformational change and "power stroke". This conformational change originates from myosin light chains, rotating the actin-binding head and producing contraction of muscle. To regulate these interactions, striated myocytes organize actin and myosin into highly structured assemblies called sarcomeres (Figure 1C). Sarcomeres are semi-crystalline orientations of myosin thick filaments intercalated between actin-composed thin filaments, creating the basic contractile unit of muscle tissue [8].

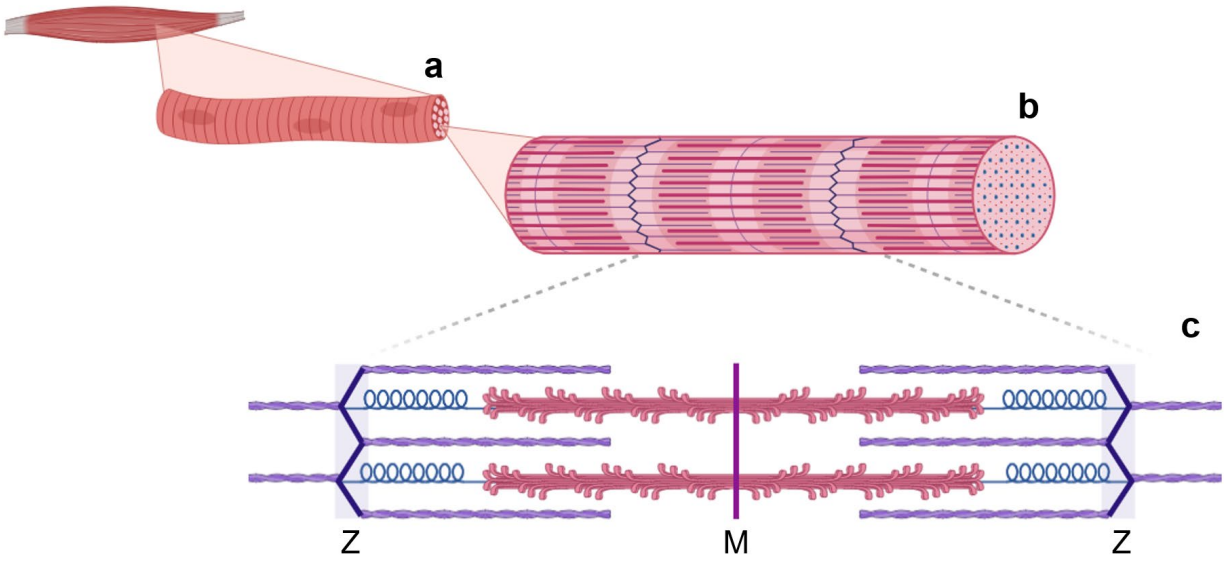

Figure 1: Diagram of straited muscle structure. Muscle strands (A) may be segmented into myofibrils (B), which are composed of sarcomeres (C), the fundamental unit of contraction. Sarcomeres contain actin "thin" filaments (purple), which slide against myosin-thick filaments (red). Passive tension is created by the giant protein titin (blue), which connects thin filaments at the Z line to M line-centered thick filaments. (Created with BioRender.com)

Within the different muscle tissues, there are similarly unique expressions of alpha-actin isoforms, which are aptly named. Cardiac tissue is mainly composed of cardiac actin (CAA), skeletal muscle is composed of skeletal actin (SKA), and smooth muscle is composed of smooth muscle actin (SMA). The expression of these isoforms is not created from alternative splicing of preRNA but rather are separate genes present on three separate chromosomes (CAA: #15, SKA:

#1, and SMA: #10). Despite their physical separation within the genome, these three isoforms are highly conserved, with 97% - 99% sequence homology (Figure 2a) and differences primarily localized at the N-terminus (Figure 2b). Although these sequences are highly conserved, any amino acid change may be hypothesized to impact contractile function. The importance of slight changes in actin can be inferred from the high conservation of each α-actin isoform between evolutionary species. For example, with 410 million years of separation (during which time Pangea separated, Dinosaurs evolved and went extinct, and the Rocky Mountains were formed), Humans and Coelacanths still share perfectly identical protein sequences for cardiac actin (Figure 2c) [9]. This amount of conservation within isoform sequences points heavily to selective pressure against the alteration of actin. With such an ancient protein lying untouched by evolution, we are given second-hand evidence of the importance of actin protein sequence changes.

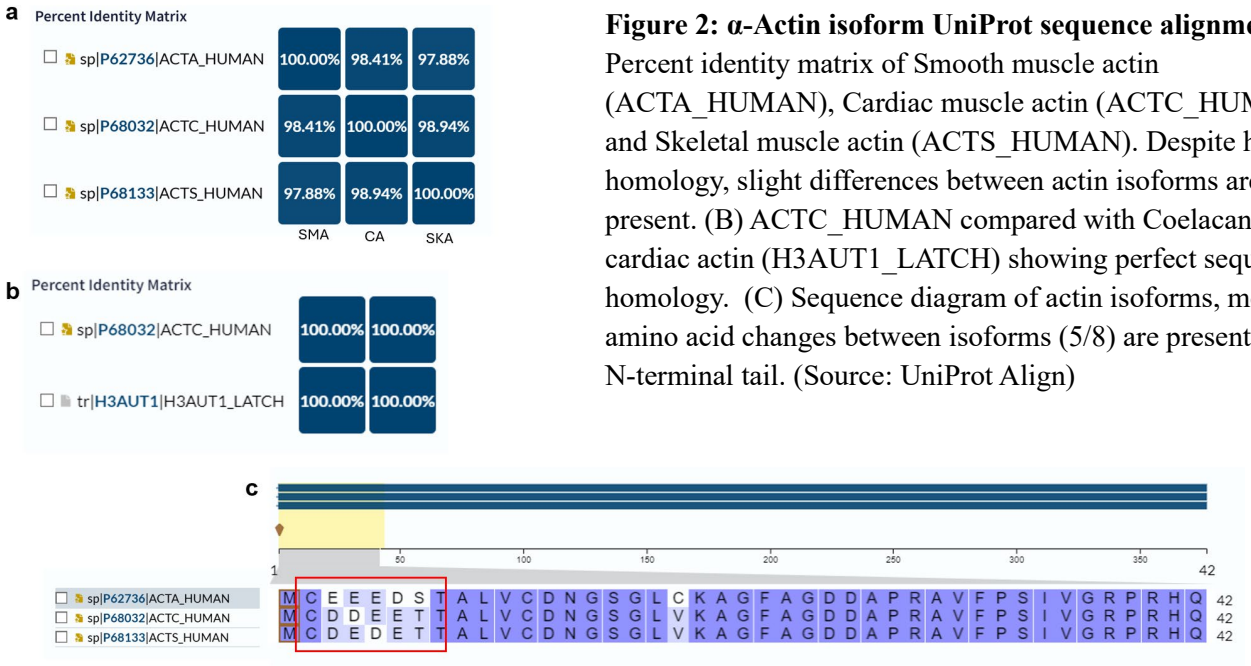

Figure 2: α-Actin isoform UniProt sequence alignment. (A) Percent identity matrix of Smooth muscle actin (ACTA_HUMAN), Cardiac muscle actin (ACTC_HUMAN), and Skeletal muscle actin (ACTS_HUMAN). Despite high homology, slight differences between actin isoforms are present. (B) ACTC_HUMAN compared with Coelacanth cardiac actin (H3AUT1_LATCH) showing perfect sequence homology. (C) Sequence diagram of actin isoforms, most amino acid changes between isoforms (5/8) are present in the N-terminal tail. (Source: UniProt Align)

Importantly for this thesis, many accessory proteins interact with actin filaments in the sarcomere to regulate the timing and strength of muscle contraction. In combination with the troponin complex (Tn), tropomyosin (Tpm) regulates myosin binding to actin. After action potentials from neurons have depolarized the cell surface, myocytes (muscle cells) release calcium stored in the sarcoplasmic reticulum (SR). This influx of calcium quickly binds to Tn,

invoking a conformational change and shifting Tpm from actin's myosin-binding sites (Figure 3a). With myosin bound to actin, contraction can occur in an ATP-dependent manner. Then, as quickly as contraction began, the Sarcoendoplasmic Reticulum Calcium ATPase (SERCA) pump begins to transport Ca++ ions back into the SR, and the cell returns to its relaxed state. This flurry of protein interactions requires highly regulated interactions and forces to ensure that myocytes can properly contract and relax. In cardiac tissue, this contractile cycle must properly cycle 60 – 100 times per minute, every minute, resulting in approximately 40,000,000 contractions each year. Importantly, this is the model for contractile regulation in striated muscle primarily composed of alpha skeletal actin (α-SKA) and alpha cardiac actin (α-CAA). Smooth muscle is primarily composed of alpha smooth muscle actin (α-SMA) and is regulated through calmodulin activation of myosin light chain kinase (MLCK), which phosphorylates the myosin regulatory light chain (RLC) and unblocks actin-binding sites under Ca++ influx (Figure 3b) [8].

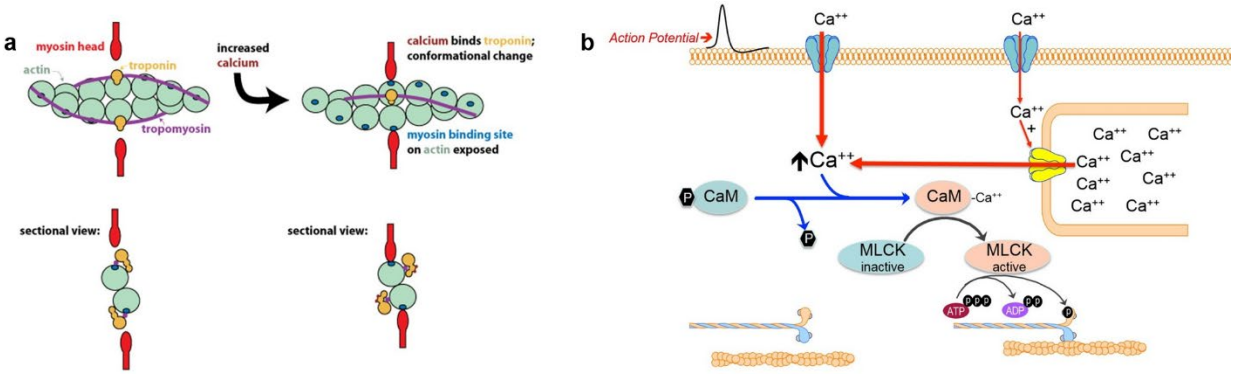

Figure 3: Comparison of striated and smooth muscle contraction mechanism. (A) Striated muscle has tropomyosin and troponin moved from myosin binding sites with calcium binding to troponin, allowing for contraction [10].**(B)** Smooth muscle generally has calcium regulated through calmodulin, and activation of myosin light chain kinase phosphorylates myosin, leading to activation. [11]

Importantly for this thesis, there are many accessory proteins that interact with actin filaments in the sarcomere to regulate the timing and strength of contraction. In combination with the troponin complex (Tn), tropomyosin (Tpm) regulates myosin binding to actin. After action potentials from neurons have depolarized the cell surface, myocytes (muscle cells) release calcium stored in the sarcoplasmic reticulum (SR). This influx of calcium quickly binds to Tn, invoking a conformational change and shifting Tpm from actin's myosin-binding sites (Figure 3a). With myosin bound to actin, contraction can occur in an ATP-dependent manner. Then, as

quickly as contraction began, the Sarcoendoplasmic Reticulum Calcium ATPase (SERCA) pump begins to transport Ca++ ions back into the SR, and the cell returns to its relaxed state. This flurry of protein interactions requires highly regulated interactions and forces to ensure that myocytes can properly contract and relax. In cardiac tissue, this contractile cycle must properly cycle 60 – 100 times per minute, every minute, resulting in approximately 40,000,000 contractions each year. Importantly, this is the model for contractile regulation in striated muscle primarily composed of alpha skeletal actin (α-SKA) and alpha cardiac actin (α-CAA). Smooth muscle is primarily composed of alpha smooth muscle actin (α-SMA) and is regulated through calmodulin activation of myosin light chain kinase (MLCK), which phosphorylates the myosin regulatory light chain (RLC) and unblocks actin-binding sites under Ca++ influx (Figure 3b) [8].

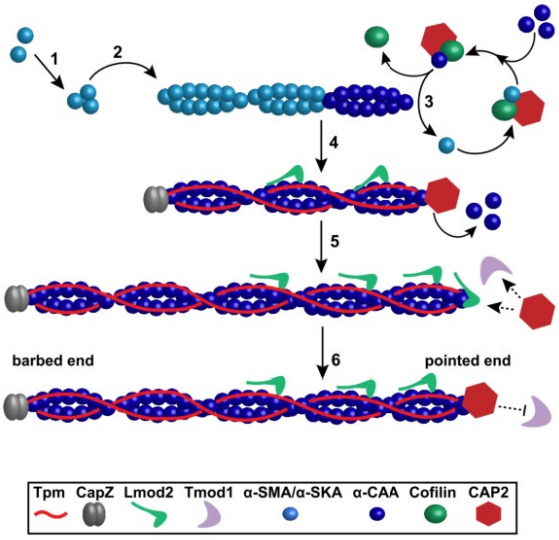

Figure 4: Model of CAP2-mediated thin filament maturation. In this model of thin filament maturation, smooth muscle and skeletal actin (α-SMA & α-SKA) are replaced with cardiac actin (α-CAA) through CAP2-mediated exchange. [1]

Adenylyl Cyclase-Associated Protein 2's (CAP2) Function in Filament Maturation

CAP2 is an actin-binding protein that localizes to the center of sarcomeres (M-line) and the pointed ends of thin filaments [12]. Functionally, CAP2 has been shown to delay actin incorporation to thin filaments, working as an actin depolymerizing protein to remove filamentous actin (F-actin) from the pointed end [12]. However, CAP2 is not a solely depolymerizing protein but also seems to have a role in adding actin monomers to the pointed end by preferentially replacing α-SMA and α-SKA with α-CAA. CAP2 also has important cellular functions in governing gene regulation through MRTF/SRF signaling pathways [13],

affecting a variety of downstream targets. In studying the effects of CAP2-KO's we see that mice develop dilated cardiomyopathy (DCM) and have dramatically reduced lifespans, display disorganized sarcomeric patterns, and importantly for this thesis, a dramatically changed distribution of α-actin isoforms within the heart (Figure 5) [12, 14, 15]. This change of actin isoform expression is likely indirectly mediated through CAP2 and MRTF/SRF signaling but indicates a potential mechanism for cardiovascular disease in these CAP2-KO mice. As I will discuss throughout this thesis, these changes in actin isoforms within cardiac tissue may contribute to the diseased state of Cap2-KO hearts, a unique mechanism that has not been previously described. Altered actin expression under loss of CAP2 is therefore a unique disease phenotype to study in mouse model, which also provides insight into a mutation known to cause disease in human patients [16-18]

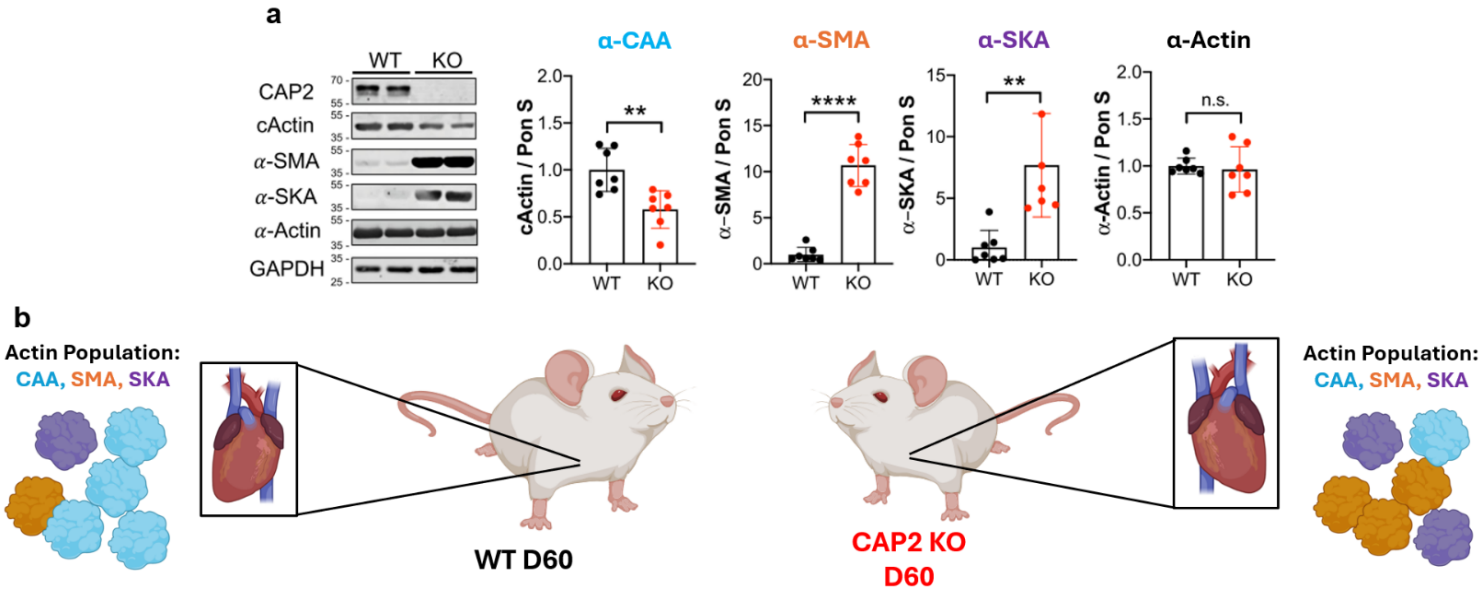

Figure 5: CAP2 mice display an altered α-actin isoform profile. (**A**) Western blot analysis from LV tissue of WT (black) or Cap2-KO mice (red) at postnatal day 60 [12]. (**B**) Cartoon diagram displaying altered actin isoform populations with unchanged total actin amounts. (Created with BioRender.com)

Similar to mice with a CAP2-KO mutation, human patients who have mutations within the CAP2 gene present with cardiovascular disease and DCM [16-18]. In the first recorded case, a 5-year-old patient with a CAP2 mutation required numerous daily medications and was placed

on a waiting list for a donor heart [16]. By better understanding the DCM disease mechanisms in CAP2-KO hearts, future research towards generating novel treatments is made possible.

RESULTS

CAP2-KO Reduced Force is Rescued with Cardiac Actin. Previously, it has been shown that the loss of CAP2 is detrimental to proper cardiovascular function in mouse models and human patients ([12, 14-16]). In one study [12] a distinct alteration in the actin isoform profile was described, where α-SMA and α-SKA protein levels were significantly higher in CAP2-KO cardiac tissue, and α-CAA protein levels were significantly decreased. This provides correlative evidence that altered α-actin isoforms (and specifically decreased α-CAA) are associated with cardiac dysfunction, which is further investigated here. To characterize the CAP2-KO disease phenotype and test the effects of increasing α-CAA at the sarcomeric level, single-cell mechanics (SCM) was used to measure individual cardiomyocyte force production and the impact of α-CAA overexpression in CAP2 cardiomyocyte force production.

Figure 6 demonstrates that A) CAP2 KO cardiomyocytes (KO) display reduced force at the single cell level, and B) the overexpression of cardiac actin can rescue the decreased contractile force observed in the KO. At maximally activating calcium, KO cardiomyocytes had markedly decreased forces at ~16.3 mN/mm^2, and a significantly different Ca^{2+} response curve compared to maximal WT forces of ~23.1 mN/mm^2 (Figure 6). Upon overexpressing α-CAA in a CAP2 KO mouse (KO + α-CAA), cells returned to near WT maximal forces (Figure 6b) at ~23.9 mN/mm^2 and were significantly different from the KO Ca^{2+} response curve (Figure 6a). WT and KO mice were injected with GFP vectors to control for the effects of injection and viral load.

These results illustrate that CAP2-KO cardiac dysfunction is present at the individual cell level, displayed as a reduction in force production at maximal calcium concentration. KO + α-CAA seems to rescue single cell force production, supporting the hypothesis that α-Actin isoform expression contributes to the *CAP2* KO disease phenotype.

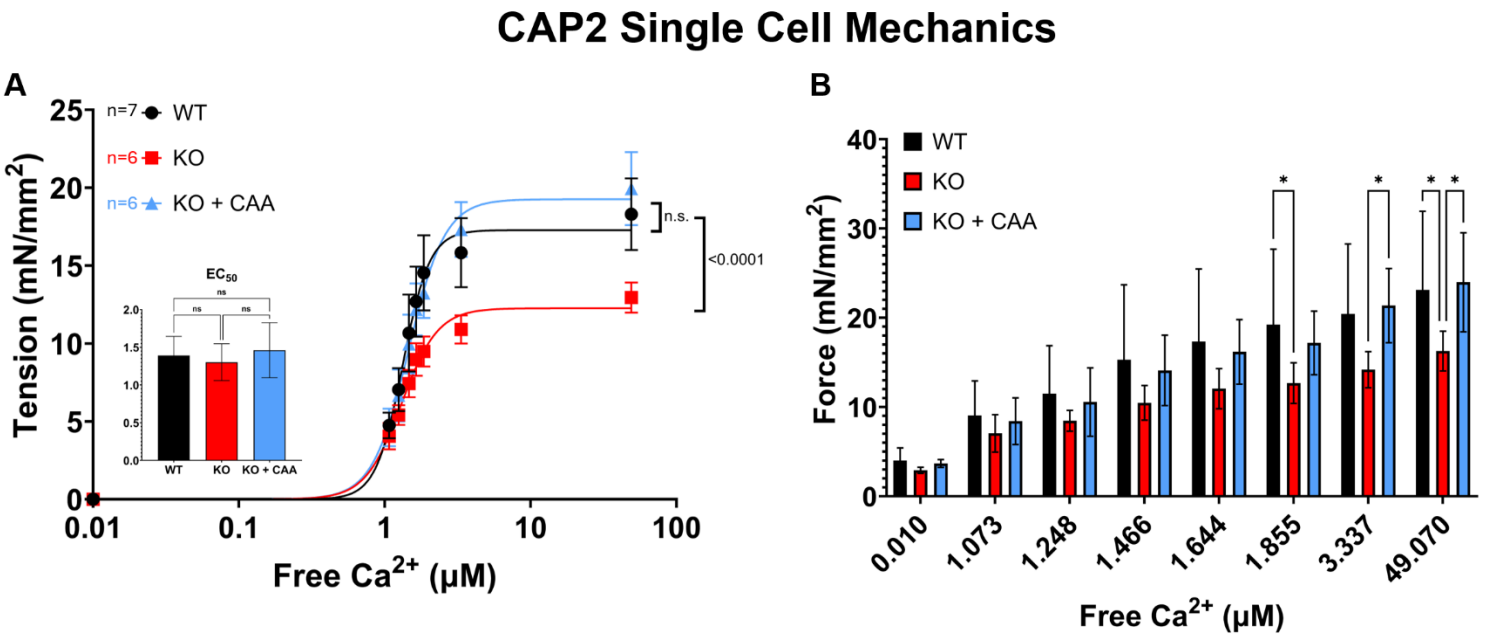

Figure 6: CAP2-KO mice have decreased force production rescued by cardiac actin. (A) Ca^{2+} dose response curves of CAP2-KO mice transfected with GFP (KO), wild-type mice transfected with GFP (WT), and CAP2-KO mice transfected with GFP-cardiac actin (KO + α-CAA). "Tension" indicates forces subtracted from low Ca^{2+} passive force (0.01uM Ca^{2+}) to allow for curve fitting. (B) Bar plot comparison of WT, KO, and KO + α-CAA forces. All transfections utilized an adeno-associated virus (AAV) vector with cardiac-specific promotor to ensure expression solely in cardiac tissue. WT and CAP2 mice were injected with GFP AAV to control for transfection and injection. *$p < 0.05$; All values are means ± SD.

Regulated α-actin isoforms are distinct *in-vitro*. In previous research, α-cardiac actin (α-CAA) and α-skeletal actin (α-SKA) were closely examined and compared in biochemical and functional assays [19-21]. In contrast, α-smooth muscle actin (α-SMA) has gone largely unstudied, and there is a distinct lack of information about how α-SMA behaves in comparison to α-CAA and α-SKA. Functional differences between α-actin isoforms may explain CAP2-KO cardiac dysfunction, with increased α-SMA/α-SKA in cardiac tissue decreasing force production or a decrease of α-CAA reducing maximal force.

To discern if the deficit in the force production in CAP2-KO hearts is due to an impaired actin-myosin interaction, we first ran IVM with fluorescently labeled α-SMA/α-SKA/α-CAA at

either 25 or 50 µg/mL. As shown in Figure 7, there are no significant differences in the sliding velocities of the actin isoforms at either myosin concentration. This indicates that the reduction in force is not due to direct changes in the actin-myosin interaction.

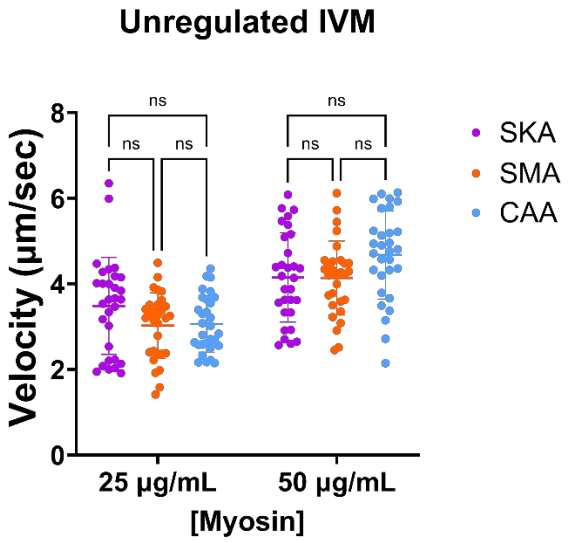

Figure 7: Unregulated actin isoforms display no changes in sliding velocity. *In-vitro* motility assay comparing unregulated SKA, SMA, and CA with points at 25 and 50ug/mL of Myosin. All IVM experiments described in this thesis were ran at 25ug Myosin.

Next, *in-vitro* motility (IVM) assays were run using reconstituted regulated thin filaments (actin, tropomyosin, and troponin complex) from purified proteins. These filaments consisted of α-actin from one of the three α-actin isoforms (SKA, CAA, or SMA) incubated with tropomyosin (Tpm) and cardiac troponin complex (cTn) placed on a bed of α-myosin, giving a physiologically relevant, calcium-regulated complex to study actin-myosin interaction.

The results from the calcium-dose response curves using the three different actin isoforms showed there were significant differences between the calcium responses of the three α-actin isoforms (Figure 8). This result shows that the regulated thin filaments have unique responses to calcium doses, suggesting that they do not play redundant roles. Comparing sliding velocities at individual calcium points (Figure 8b), α-SKA and α-CAA had similar velocities at saturating calcium (49µM), whereas α-SMA showed a significant decrease in sliding velocity. This indicates decreased interactions between α-SMA and myosin, compared to α-SKA and α-CAA at high calcium and may be explained by altered interactions with cTn and/or Tpm. At lower levels of calcium (~1µM), the three isoforms had significantly distinct average sliding velocities (Figure 8b). Skeletal actin had the fastest sliding velocity, followed by smooth muscle actin and cardiac actin. Because CAP2-KO leads to an increase in α-SMA and α-SKA but an

overall decrease in force production in cardiac tissue, an early hypothesis was that *α-SKA and α-SMA had decreased actin-myosin interactions compared to α-CAA*. However, this result suggests that α-SMA may play a larger role in decreasing contractile force at maximal [Ca2+] compared to SKA and that the effect of isoforms may also be due to altered calcium regulation. Upon quantifying the EC_{50} of the fitted modified Hill curve (Equation 1, Methods), there were non-significant trends of a lower EC50 of both α-SKA and α-SMA (Figure 8, Inset).

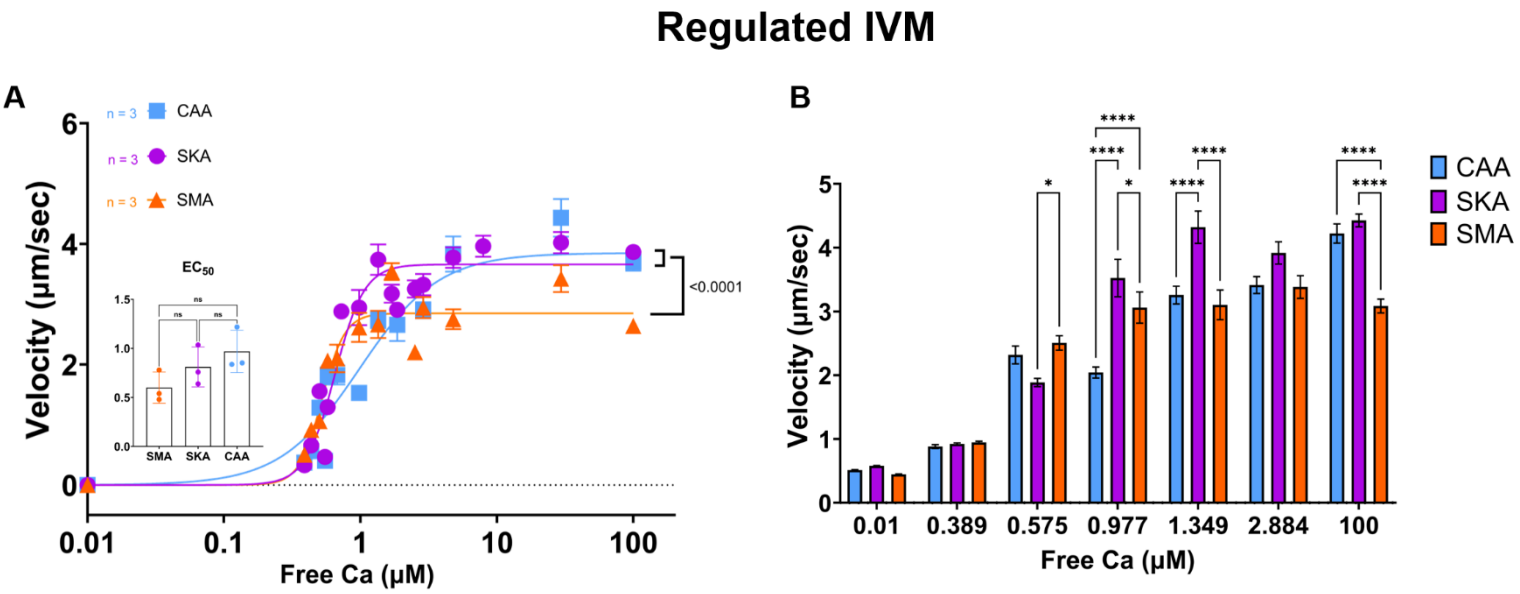

Figure 8: Regulated thin filaments of SMA have reduced myosin interactions. (A) Calcium dose-response curves with actin isoforms regulated with Tpm and cTn. Dose response curve fits are significantly different. (B) Bar plot of filament velocities at calcium concentrations. Calcium concentrations chosen where all 3 isoforms had >20 video recordings. *$p < 0.05$; ****$p < 0.0001$; Averages ± SEM.

cTn shows Unique Binding Affinity to Actin Isoforms. *In-vitro* motility assays demonstrate that bare actin filaments do not have significantly different actin-myosin interactions, but regulated filaments are significantly different. To test the hypothesis that SMA binds differently to Tpm & cTn to "cripple" myosin interactions, co-sedimentation assays were performed. Co-sedimentation assays can be used to ascertain the binding affinity of actin-binding proteins [22], allowing us to quantify the binding of cTn and Tpm to each of the actin isoforms. We predict that

these regulatory proteins bind differently to Smooth Muscle Actin, providing a molecular mechanism by which force is altered *in vitro* and at the single-cell level.

We first tested if tropomyosin has an altered binding to the actin isoforms. Co-sedimentation assays were run with actin isoforms and Tpm alone (Figure 9a), where Tpm was incubated overnight with f-actin isoforms. The solution was then centrifuged to pull down polymerized actin, forming a pellet that also contains any f-actin bound tropomyosin. Upon quantification, the amount of Tpm pulled down with each of the actin isoforms was unchanged (Figure 9a). This result suggests that SMA, SKA, and CAA do not have different binding affinities to Tpm.

To test the binding affinity of cTn, purified cTn and Tpm were incubated with each of the f-actin isoforms (α-SMA, α-SKA, and α-CAA). Similar to Tpm-only co-sedimentation assays, cTn and Tpm were incubated with each of the f-actin isoforms overnight. Each actin-Tpm-cTn mixture was then centrifuged to form pellets of F-actin, which also contain any bound Tpm and cTn. Figure 9b shows the ratios of cardiac troponin subunits (cTnI, cTnT, and cTnC) and Tpm, normalized to the f-actin present in each pellet. Strikingly, the α-SMA pellet contains much higher amounts of cTnT and cTnI compared to what is observed in the α-SKA and α-CAA pellets (Figure 9b), suggesting that these regulatory proteins have higher binding affinity for α-SMA compared to α-SKA and α-CAA. Compared to skeletal actin, α-SMA pellets also have a significantly higher association with Tpm which is also trended in the α-CAA pellets, though it is not significant ($p=0.07$). The altered binding affinities between actin isoforms with Tpm/cTn suggest that the troponin complex is responsible for different binding affinities, which may also regulate the association of Tpm. This cooperative nature between Tpm and cTn is known to exist [23], explaining why Tpm also has increased binding to α-SMA when incubated alongside cTn (Figure 9b).

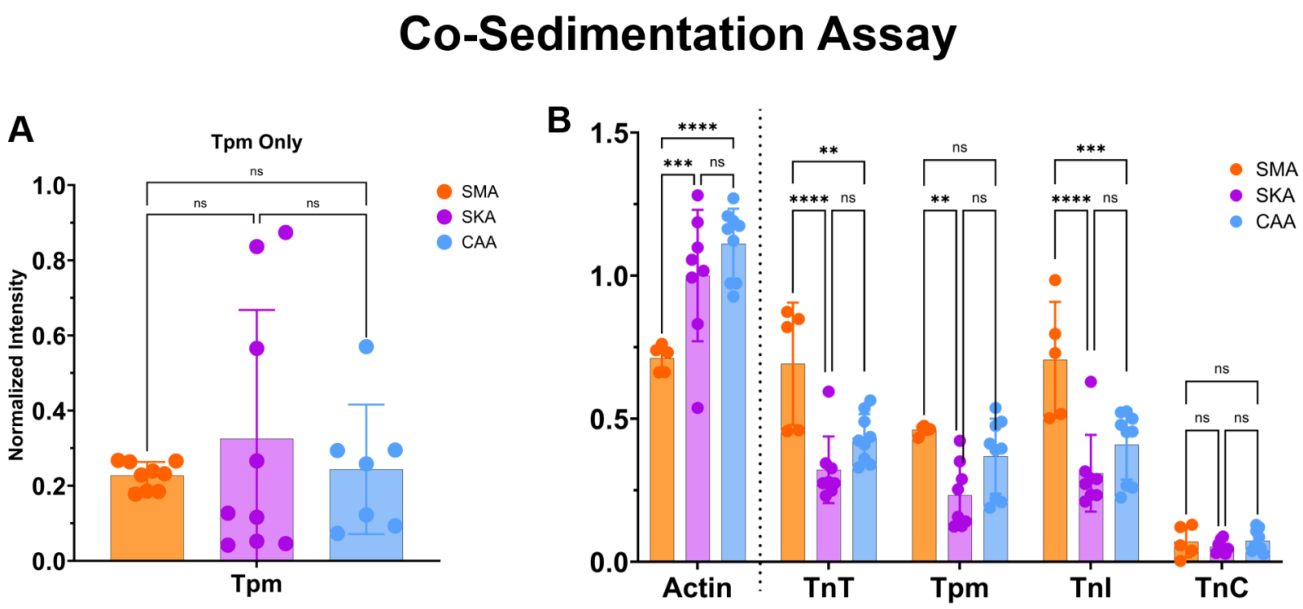

Figure 9: SMA displays increased cTn binding affinities compared to SKA and CAA. (A) Bar plot with Tpm-only co-sedimentation, describing the relative amount of Tpm that was pelleted with each actin isoform. (B) Co-sedimentation assay showing the percentage of actin in the pellet (i.e., F-actin), as well as the amount of Troponin T (TnT), Troponin I (TnI), Troponin C (TnC), and Tropomyosin (Tpm) in the pellets. All protein concentrations were normalized to the total amount of actin present in the pellet, with actin bands normalized to non-centrifuged actin. Averages +/- SD.

These results support the hypotheses that *α-actin isoforms change contraction through altered regulatory protein interactions, specifically cTn's increased binding affinity to α-SMA*. With increased binding to cTn, which is not expressed in smooth muscle tissue, α-SMA's myosin interactions under calcium concentrations are reduced, resulting in lower overall sliding velocity.

CONCLUSIONS

In this thesis, I compare the properties of alpha-actin isoforms and their effects on contraction within cellular and *in-vitro* environments. The disease phenotype in the absence of Cap2 (CAP2 KO) includes decreased cardiac output as measured by ejection fraction, pathological phenotypes such as ventricular dilation, and the development of dilated cardiomyopathy (DCM) [12, 14-17]. Due to CAP2's role in actin dynamics, alterations in the alpha-actin population have been shown in CAP2 KO mice, resulting in higher concentrations of

SMA and SKA (Figure 4). Previous literature has explored the role of smooth muscle actin concerning cardiogenesis in development [24] [25] or bare SMA filaments [26], but there was previously a lack of research describing mechanical and contractile properties of regulated SMA.

In measuring the force production of individual cardiomyocytes with SCM, a dramatic decrease in force was shown with CAP2-KO cells (16.3 mN/mm^2) compared to WT cells (23.1 mN/mm^2). Upon overexpression of alpha-CAA in CAP2-KO cells, force was recovered to near-WT levels (23.9 mN/mm^2), providing evidence that reduced cardiac actin may drive decreased force production rather than being a byproduct of the overall disease (Figure 6). To further study this hypothesis in an *in vitro* controlled environment, actin-myosin interactions for each unregulated and regulated alpha isoform were measured via IVM assays (Figures 7 & 8). In line with previous literature [26], unregulated SMA, SKA, and CAA had no significantly different sliding velocities (Figure 7), meaning that there was no apparent difference in actin-myosin interaction between alpha-actin isoforms. In contrast, regulated actin isoforms (i.e., f-actin bound with Tpm and cTn) displayed distinct Ca^{2+} dose response curves with regulated SKA and CAA having significantly faster sliding velocities (~ 3.9 & 3.71 μm/sec, respectively) in comparison to SMA (2.64 μm/sec) at saturating calcium (Figure 8).

Evidence from these experiments, therefore, points to a changed actin-myosin interaction from alpha-actin isoforms' differential interactions with thin filament regulatory proteins cTn and/or Tpm. To characterize the binding of cTn and Tpm to the actin isoforms, co-sedimentation assays were run (Figure 9a). We have shown that α-SMA pulls down significantly more cTnT and cTnI compared to SKA and CAA, as well as increased Tpm compared to SKA. Upon further dissection of these interactions, it was shown that Tpm alone does not bind differentially to any of the actin isoforms (Figure 9b). These results further support that α-actin isoforms have functional differences in muscle contraction, likely mediated through differential cTn binding. An inference from these data is that cTn has an increased binding affinity to SMA in low Ca++ conditions, resulting in a tighter blocking of myosin binding sites when calcium is present. This increased binding affinity would tamper with the delicate regulation of contraction, where cTn must have strong enough binding with actin's myosin binding sites to block contraction without calcium. Once calcium is released and bound, the conformational changes in the open position must be energetically favorable enough to reveal actin's myosin binding sites. Therefore, with

increased binding affinity in the calcium free state, the conformational shift for activation would become slightly less favorable, Tpm shifting times increase (or overall rates decrease), and the sliding velocity of the filament is reduced.

DISCUSSION AND FUTURE DIRECTIONS

Although sequence homology is high between the alpha-actin isoforms, the slight differences within the N-terminus of actin may explain these isoform differences. The N-terminal tail of actin is typically disordered, making it difficult to visualize in structural studies such as Cryo-EM [21] but has been previously implicated in many functions. One such structural study on actin isoforms (including alpha-SKA and CAA, but not SMA) predicted the N-terminus to impact actin-myosin loop 2 interactions when myosin-bound ([21], Figure 7). Actin's N-terminus has also been implicated in binding to Troponin I [27], where cTnI would inhibit a myosin binding site. Combined with results presented in this thesis, it is reasonable that SMA's altered N-terminus is responsible for an increased binding affinity for cTn and may directly (or via Tpm) reduce myosin head binding. With Cap2 removed, an increase in SMA expression leads to the incorporation of SMA into the cardiac thin filament, which may be responsible for a portion of the disease phenotype. With Cap2's many cellular roles [28] it is highly unlikely that dysregulated actin isoform switching is solely responsible for the disease phenotype, but this actin isoform switching seems to have a meaningful impact.

Studying actin and myosin interactions in a controlled environment demonstrates that impairment is not caused directly by actin-myosin interactions but rather through actin and the associated regulatory proteins. By using IVM and Co-sedimentation assays, the interactions between actin, myosin, and purified regulatory proteins can be tested, allowing for more precise and interpretable data. However, controlling biological variation leads to a limitation of this study, the lack of external factors (such as post translation modifications) on the model system. These post-translational modifications can have significant impacts; therefore studying systems *in-vivo* is also crucial. As a separate, more minor limitation of this thesis, although quasi-binding coefficients can be calculated from co-sedimentation assay data [22], this requires running concentration curves for each of the actin binding proteins in question (i.e., cTn & Tpm). Due to time limitations and the difficulty in purifying SMA, inadequate SMA was available for running

multiple binding curves, and therefore, co-sedimentation assays were run at consistent concentrations of cTn and Tpm. This limits the quantification of binding affinity between the actin isoforms and cTn/Tpm but does not invalidate the results presented here.

In continuing this work, there are several questions still unanswered. Further investigation on the structural differences between alpha-actin isoforms may help answer why actin isoforms interact differently with accessory proteins. X-ray diffraction of Cap2 muscle tissue could give insight into differences in the placement of cTn/Tpm or shifting of actin within the sarcomere. Improvements in the purification of Smooth muscle actin protocols would also be a worthwhile research goal to allow for easier future investigation of the alpha actin isoforms in biochemical and *in-vitro* studies. With optimized SMA purification protocols, full characterization of binding affinities and dissociation constants (Kd) for cTn and Tpm could be calculated and compared with binding to alpha SKA and CAA isoforms.

Another question that remains is why the increased expression of SKA is not able to rescue the CAP2-KO disease phenotype. With the experiments described here, it may be hypothesized that an overexpression of SKA would replace CAA's role within the thin filament and rescue contractile forces. A possible explanation for this is that SKA does alleviate aspects of the CAP2-KO disease phenotype but is not highly expressed enough to rescue decreased force fully. Therefore, we predict that an over-expression of SKA in a CAP2-KO mouse should replicate the results seen in CAP2 + CAA single cell mechanics experiments, rescuing force production. Another experiment to validate findings here would be an overexpression of SMA in a WT mouse, which is predicted to sharply decrease force production. Each of these questions would further test the impact of alpha-actin isoforms on the function of cardiomyocyte contraction and give insight into a previously unstudied mechanism of cardiovascular disease.

METHODS

Single Cell Mechanics (SCM)

By day 4, WT mice were injected with cTnT-AAV-GFP as a control, and at the same time, Cap2 KO mice were injected with either the same control virus or a cTnT-AAV-GFP-

αCAA virus. These mice were allowed to age up to day 62-75, whereby the hearts were excised out, and the right ventricle (RV), left ventricle (LV), and intraventricular septum (IVS) were separated into different tubes and flash-frozen in liquid nitrogen. The cardiac TnT promoter was used to ensure expression of the cardiac actin only in the hearts. Single-cell mechanics (SCM) was performed with interventricular septum cardiac tissue from male mice.

All solutions used for SCM were made as previously described [29]. Single-cell experiments were performed on an inverted microscope stage using an Aurora Scientific 803B permeabilized myocyte apparatus with some slight modifications; a 406A force transducer was used to obtain a wider range of minimum and maximum forces. Tissue samples were broken from frozen interventricular septum (IVS) samples and immediately placed into 1% Triton X-100 skinning solution. The tissue was then disrupted using a rotor-stator-homogenizer for 5-7x 1s bursts. The cells were gently pelleted by centrifugation for 3 min at 20 g. The supernatant containing the skinning solution was removed, and the pellet was washed with a relaxing solution to remove any remaining detergent, with centrifugation and washing steps repeated three times.

Two stock solutions containing either 49mM Ca^{2+} or 0.01 mM Ca^{2+}, herein referred to as activating and relaxing solutions, are mixed to generate a total of 8 Ca^{2+} doses. To control for selection bias and ensure against temporal confounding variables, all SCM experiments had a randomized order for the Ca^{2+} solutions used. Similarly, the order of experiments for WT, CAP2 KO, and CAP2 KO + cActin cells were randomized.

SCM experiments were performed as previously described [29]. In brief, a microscope slide is placed in the inverted microscope stage with coverslips containing the disrupted cardiomyocytes and a thin strand of silicone adhesive. Dual controllers are used to maneuver the force transducer and motor arm, apply glue, and adhere to a skinned cardiomyocyte (Supplemental Figure 1) before curing in a relaxing solution for 30 minutes. Cell length measurements are selected in the Aurora software from cell edge to edge (Supplemental Figure 1, red lines), with this distance recorded as Length out (Lo) = 1. Cell thickness was estimated as ½ of cell width at slack length. Before activation, cells were stretched to a diastolic sarcomere length of 2.25 – 2.30μm.

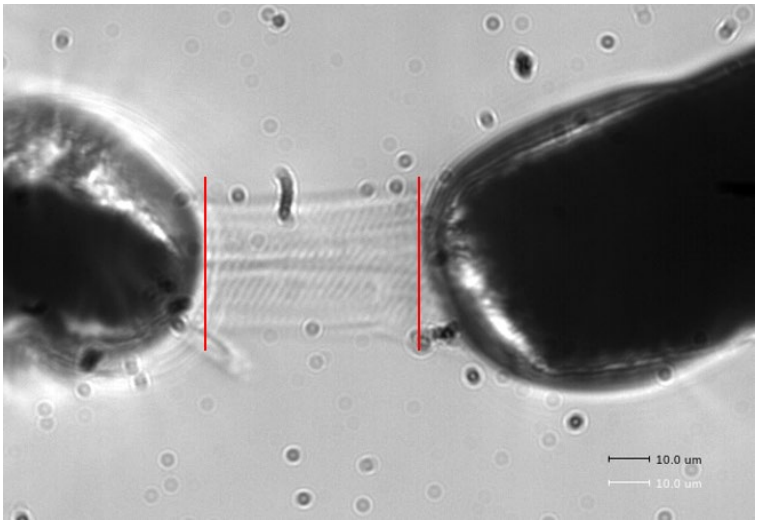

Supplemental Figure 1: Example image of skinned cardiomyocyte. This cardiomyocyte is attached to a 406A force transistor (left) and motor arm (right). Red lines denote the cell length measurement points, where the distance between is standardized to 1 Length (Lo). The cell shown was collected from Mouse 408, CAP2 KO + CAA.

To measure forces throughout calcium concentrations, the glued cardiomyocyte was moved between the relaxing buffer to the desired [Ca^{2+}] buffer. Once peak force plateaued, a step release was performed by moving the motor arm to Lo = 0.65, creating a peak tension to a minimum force. The difference in measured force between the plateau and subsequent step release is the total force generated by the cell. A cell's force generated while in a calcium-free buffer (Passive) is subtracted off, resulting in a cell's net Active Tension, the reported measurement here. This method, therefore, normalizes force for each cell's underlying passive tension.

The resulting calcium curves were fit individually to a modified Hill equation as previously described [30]:

$$Fre1 = F_{max} * (x^{HillSlope}) / ((x^{HillSlope}) + (LogEC_{50}{}^{HillSlope}))$$

Where the F_{max} is the force at saturating [Ca^{+2}], EC_{50} is the [Ca^{+2}] where Force is half of F_{max}, HillSlope is the Hill slope, and x is the [Ca^{+2}].

IVM:

The solution composition, as shown in Table 1, and flow cell loading were performed as previously described with some modifications [[31], [32]]. An HDTA-based actin buffer was used to remove all residual EGTA within the flow cell, thereby standardizing Ca^{2+} concentrations before adding motility buffer at the desired pCa. Briefly, a flow cell is made by laying down three strips of double-sided sticky tape onto a glass slide creating two "lanes" that will be enclosed by the glass coverslip that had been coated with nitrocellulose. Adding solutions into the flow channel of the experimental chamber, gravity and capillary action will draw the solution into the flow cell. For a 22 x 22mm coverslip, the volume of the flow cell is ~20–25 µL and is referred to here as 1 volume. To load the flow cell, first add 1 Volume of 25 µg/mL of myosin and incubate for 1 min before the addition of 1 volume of 1 mg/mL of BSA to coat non-myosin-bound surfaces and to prevent nonspecific binding of the actin filaments. 1µM unlabeled actin is then added to the flow cells to block non-cycling myosin heads, which would prevent labeled actin filaments from sliding properly. This actin is then removed with 2 volumes of Actin-ATP buffer (allowing for myosin heads to cycle) followed by 4 Volumes of Actin buffer to restore the chamber to a rigor state. The labeled regulated actin is added to the flow cells and incubated for 5 minutes. Any EGTA/Ca^{2+} present is cleared with an HDTA-based buffer added to the flow cells, followed by a two-minute incubation of troponin & tropomyosin to ensure excess regulatory

Compound	Myosin Buffer	Actin Buffer EGTA	Actin Buffer HDTA	Actin + ATP	Motility Buffer pCa 10	Motility Buffer pCa 4	Tm/cTn Wash
KCL	300 mM	55 mM	55 mM	55 mM	55 mM	40 mM	55 mM
BES	25 mM	25 mM	25 mM	25 mM	25 mM	25 mM	25 mM
$MgCl_2$	4 mM	4 mM	4 mM	4 mM	4 mM	4 mM	4 mM
$CaCl_2$	0 mM	0 mM	0 mM	0 mM	0 mM	5.09 mM	0 mM
HDTA	0 mM	0 mM	5 mM	0 mM	0 mM	0 mM	0 mM
EGTA	5 mM	5 mM	0 mM	5 mM	5 mM	5 mM	5 mM
Glucose	0 mM	0 mM	0 mM	0 mM	2 mM	2 mM	0 mM
ATP	0 mM	0 mM	0 mM	1 mM	1 mM	1 mM	0 mM
DTT	1 mM	1 mM	1 mM	1 mM	1 mM	1 mM	1 mM
Glucose oxidase	N/A	N/A	N/A	N/A	160 units	160 units	N/A
Catalase	0 µM	0 µM	0 µM	0 µM	2 µM	2 µM	0 µM
Tm	0 nM	0 nM	0 nM	0 nM	300 nM	300 nM	300 nM
cTn	0 nM	0 nM	0 nM	0 nM	300 nM	300 nM	300 nM

proteins for measured actin filaments. Finally, motility is induced with the addition of ATP and measured amounts of free Ca^{2+} (1 mM and 0.01μM - 100μM, respectively).

Table 1: IVM Buffer Solutions. *Composition of the buffers and solutions used in IVM experiments.*

Smooth Muscle Actin Purification:

Smooth muscle actin was extracted from Bovine aorta and purified as previously described [33], with slight modifications. Bovine aorta was previously processed and dried into acetone powder. 10 volumes (i.e., 1ml/1g tissue) of extraction buffer (2mM HEPES, 0.2mM CaCl2, 0.2mM ATP, and final pH 7.8) were mixed with Bovine aorta acetone powder and stirred at 4° C for 30min. Crude α-SMA extract was filtered from tissue with Whatman filter 1, and large particulates were spun out of the solution (10,000g, 10min). This filtered extract was then concentrated via a centrifugal concentrator (Vivaspin 10kDa, Aubagne Cedex, FR) before 100mM KCl was added and left to polymerize actin (2hr, RT). 1mM EDTA was added, and KCl concentration was increased to 800mM to dissociate Tpm from polymerized actin, before ultracentrifugation (40,000g, 1hr) to pellet polymerized actin. Pelleted polymerized actin was washed and resolubilized in an extraction buffer with gentle pipette mixing and sonication on ice. Actin was depolymerized via dialysis against an extraction buffer overnight twice (4° C). After dialysis, α-smooth muscle g-actin was clarified via ultracentrifugation (400,000g, 45min) twice. SDS-PAGE of smooth muscle actin showed a single major protein band with minor contaminants visible only when the actin was overloaded.

Co-sedimentation Assay:

Co-sedimentation assays were run as previously described [22], with slight alterations. To control for differences in protein behavior in altered solution conditions, the polymerization buffer was substituted with EGTA Actin Buffer (Table 1). Protein ratios of 4 phalloidin-stabilized actin: 1 Tpm: 1 cTn were used, with concentrations of 4uM Actin: 1uM Tpm/cTn. Tpm was incubated with actin filaments at 4C for 8 hours before incubating with cTn overnight at 4C. For Tpm-only co-sedimentation assays, identical ratios of proteins were used, but cTn was excluded, and Tpm was incubated overnight. Samples were centrifuged at 100,000 x g for 30 minutes before separating supernatant from pellet, resolubilizing pellet with 7M Urea, 0.5% SDS, & 200

mM NaCl, and running on a 12% bis-acrylamide SDS-PAGE. The quantification of bands was performed with ImageJ [34].

Data Analysis

IVM data was analyzed with the IVM analysis software "Philament" [35], a Python-based software that was developed for high-throughput video analysis. Tracking Memory was set to 5 frames (corresponding to 1 second, with 5 FPS) and Object Diameter = 35. Recordings of IVM data at pCa 10 were analyzed with Search Ranges = 5 pixels. All other recordings were analyzed together with Search Range = 20 pixels. These data were analyzed separately because of pCa 10's reduced movement. By shrinking the Search Range, Philament is prevented from tracking incorrect "jumping" between nearby stationary filaments. Philament is tested for Windows, open-source, and available for download at https://github.com/maxwellbowser/philament.

SCM data was analyzed with a custom Python-based analysis pipeline. The "pCa_SCM_analysis.py" script automates the process of opening cell force recordings and the calculation of cell tension. This process was done in two different forms, a "manual" version and an "automated" version. After a folder name is created and a filtering value is chosen to smooth noise, the manual analysis extracts recorded cell dimensions and opens a graphical user interface (GUI) to calculate tension for a selected file (Supplemental Figure 2). The User can click and drag their mouse on any two sections of the top panel, which displays the recorded force trace for a cell. The data within each selected region is averaged, and the absolute value of the difference between the two selections is displayed on the bottom panel in μN. Once a dataset has been analyzed by hand and may be used as a ground truth, the "automated" version may be calibrated.

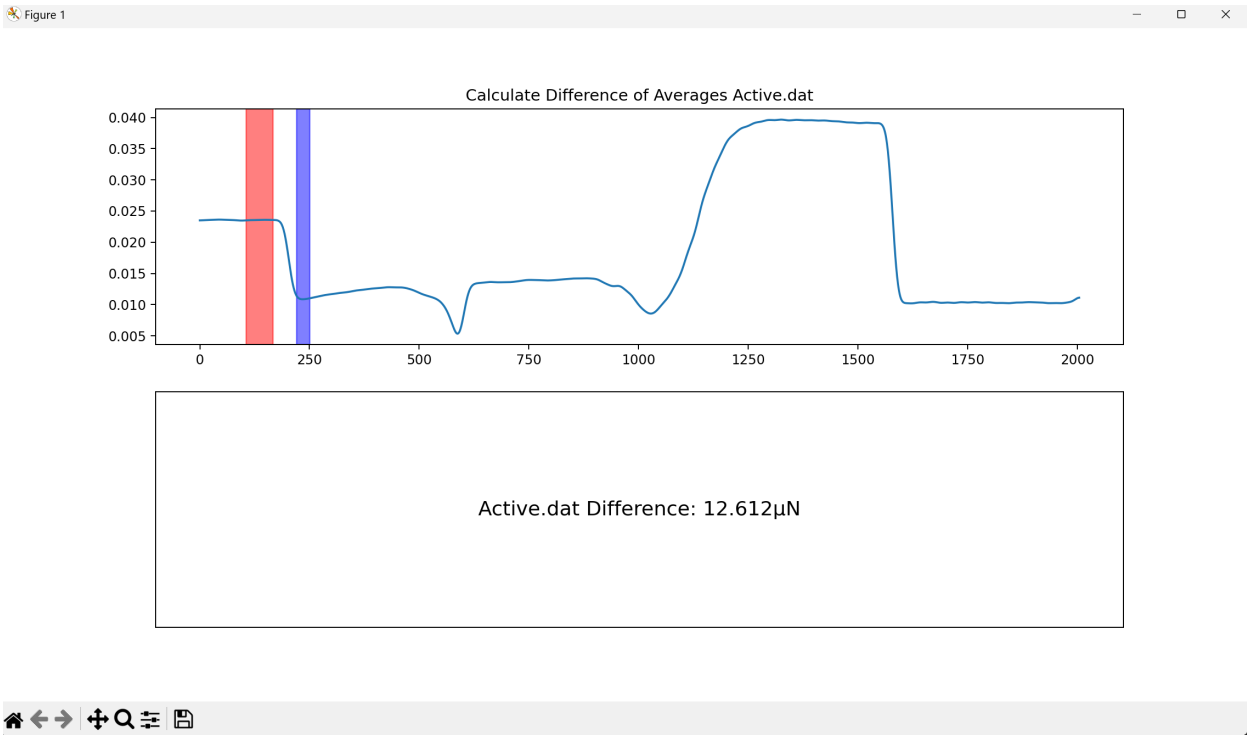

Supplemental Figure 2: Single Cell Mechanics Manual Analysis GUI. The user may select two regions of interest to find the difference. Once two regions are selected, the difference is calculated, and the absolute value is displayed on the bottom panel. "Active.dat" refers to the name of the selected file. The x-axis represents time in units depending on the force transducer sampling rate (1kHz = 1 millisecond), and the y-axis represents force in units depending on the force transducer scaling (shown here as N).

The automated SCM analysis performs identical calculations to the manual version and simply standardizes the process by selecting the same regions for all selected files every time. The difference between the averages calculated cell tensions are then formatted and saved as an Excel sheet. After testing, the optimal parameters were to average the first 200ms as a baseline, skip 40ms to account for the motor arm's movement, and finally average the following 5ms. All SCM data presented in this thesis were analyzed with this automated version, Filtering = 10. A user guide on the automated SCM_analysis.py pipeline, as well as the Python scripts and force normalization Excel sheet, is available at https://github.com/maxwellbowser/SCM_analysis.

All data analysis scripts were written, tested, and run on the Microsoft Windows 11 operating system in Python version 3.11.

Statistics

All statistical analyses were performed using Prism software (GraphPad). All statistical analyses were done using an unpaired t-test or two-way analysis of variance (ANOVA). All values are shown as mean ± SD unless otherwise specified; P-val < 0.05 was considered significant.

REFERENCES

1. Iwanski, J.B., *The Role of Pointed End Binding Proteins in Cardiac Thin Filament Actin Regulation and the Development of Dilated Cardiomyopathy*. 2022, The University of Arizona.
2. Martin, S.S., et al., *2024 Heart Disease and Stroke Statistics: A Report of US and Global Data From the American Heart Association.* Circulation, 2024. **149**(8): p. e347-e913.
3. Kazi, D.S., et al., *Forecasting the Economic Burden of Cardiovascular Disease and Stroke in the United States Through 2050: A Presidential Advisory From the American Heart Association.* Circulation, 2024. **150**(4): p. e89-e101.
4. Wilson, P.W.F., W.P. Castelli, and W.B. Kannel, *Coronary risk prediction in adults (The Framingham Heart Study).* American Journal of Cardiology, 1987. **59**(14): p. G91-G94.
5. McNally, E.M. and L. Mestroni, *Dilated Cardiomyopathy.* Circulation Research, 2017. **121**(7): p. 731-748.
6. Weintraub, R.G., C. Semsarian, and P. Macdonald, *Dilated cardiomyopathy.* The Lancet, 2017. **390**(10092): p. 400-414.
7. Schultheiss, H.-P., et al., *Dilated cardiomyopathy.* Nature Reviews Disease Primers, 2019. **5**(1): p. 32.
8. Bruce, A., et al., *Molecular Biology of the Cell*. 2014, Oxford, UNITED KINGDOM: Taylor & Francis Group.
9. Consortium, T.U., *UniProt: the Universal Protein Knowledgebase in 2025.* Nucleic Acids Research, 2024. **53**(D1): p. D609-D617.
10. Asbury, C. *Muscle physiology*. [cited 2025; Available from: https://uw.pressbooks.pub/musclephysiology/chapter/chapter-1/
11. Gordon, J. *Mechanism of smooth muscle contraction flashcards*. [cited 2025 04/09/2025]; Available from: https://quizlet.com/30216728/mechanism-of-smooth-muscle-contraction-flash-cards/

12. Colpan, M., J. Iwanski, and C.C. Gregorio, *CAP2 is a regulator of actin pointed end dynamics and myofibrillogenesis in cardiac muscle.* Commun Biol, 2021. **4**(1): p. 365.
13. Xiong, Y., et al., *Targeting MRTF/SRF in CAP2-dependent dilated cardiomyopathy delays disease onset.* JCI Insight, 2019. **4**(6).
14. Peche, V.S., et al., *Ablation of cyclase-associated protein 2 (CAP2) leads to cardiomyopathy.* Cell Mol Life Sci, 2013. **70**(3): p. 527-43.
15. Field, J., et al., *CAP2 in cardiac conduction, sudden cardiac death and eye development.* Scientific Reports, 2015. **5**(1): p. 17256.
16. Aspit, L., et al., *CAP2 mutation leads to impaired actin dynamics and associates with supraventricular tachycardia and dilated cardiomyopathy.* J Med Genet, 2019. **56**(4): p. 228-235.
17. Gurunathan, S., et al., *A homozygous CAP2 pathogenic variant in a neonate presenting with rapidly progressive cardiomyopathy and nemaline rods.* American Journal of Medical Genetics Part A, 2022. **188**(3): p. 970-977.
18. Patel, R. and R. Peterson, *Cardiomyopathy presenting prenatally with functional tricuspid and pulmonary atresia.* Echocardiography, 2019. **36**(9): p. 1779-1782.
19. Ishii, S., et al., *Myosin and tropomyosin–troponin complementarily regulate thermal activation of muscles.* Journal of General Physiology, 2023. **155**(12).
20. Kopylova, G., et al., *The properties of the actin-myosin interaction in the heart muscle depend on the isoforms of myosin but not of α-actin.* Biochem Biophys Res Commun, 2016. **476**(4): p. 648-653.
21. Arora, A.S., et al., *Structural insights into actin isoforms.* Elife, 2023. **12**.
22. Heier, J.A., D.J. Dickinson, and A.V. Kwiatkowski, *Measuring Protein Binding to F-actin by Co-sedimentation.* J Vis Exp, 2017(123).
23. Solís, C. and J.M. Robinson, *Cardiac troponin and tropomyosin bind to F-actin cooperatively, as revealed by fluorescence microscopy.* FEBS Open Bio, 2020. **10**(7): p. 1362-1372.
24. Eppenberger-Eberhardt, M., et al., *Reexpression of alpha-smooth muscle actin isoform in cultured adult rat cardiomyocytes.* Dev Biol, 1990. **139**(2): p. 269-78.
25. Clément, S., et al., *Expression and function of α-smooth muscle actin during embryonic-stem-cell-derived cardiomyocyte differentiation.* Journal of Cell Science, 2007. **120**(2): p. 229-238.
26. Harris, D.E. and D.M. Warshaw, *Smooth and skeletal muscle actin are mechanically indistinguishable in the in vitro motility assay.* Circ Res, 1993. **72**(1): p. 219-24.
27. Levine, B.A., A.J. Moir, and S.V. Perry, *The interaction of troponin-I with the N-terminal region of actin.* Eur J Biochem, 1988. **172**(2): p. 389-97.

28. Rust, M.B., et al., *CAPt'n of Actin Dynamics: Recent Advances in the Molecular, Developmental and Physiological Functions of Cyclase-Associated Protein (CAP).* Front Cell Dev Biol, 2020. **8**: p. 586631.
29. Pappas, C.T., et al., *Cardiac-specific knockout of Lmod2 results in a severe reduction in myofilament force production and rapid cardiac failure.* J Mol Cell Cardiol, 2018. **122**: p. 88-97.
30. Farman, G.P., et al., *Impact of osmotic compression on sarcomere structure and myofilament calcium sensitivity of isolated rat myocardium.* Am J Physiol Heart Circ Physiol, 2006. **291**(4): p. H1847-55.
31. Farman, G.P., et al., *Impact of familial hypertrophic cardiomyopathy-linked mutations in the NH2 terminus of the RLC on β-myosin cross-bridge mechanics.* J Appl Physiol (1985), 2014. **117**(12): p. 1471-7.
32. Farman, G.P., et al., *HCM and DCM cardiomyopathy-linked α-tropomyosin mutations influence off-state stability and crossbridge interaction on thin filaments.* Arch Biochem Biophys, 2018. **647**: p. 84-92.
33. Strzelecka-Gołaszewska, H., S. Zmorzyński, and M. Mossakowska, *Bovine aorta actin. Development of an improved purification procedure and comparison of polymerization properties with actins from other types of muscle.* Biochim Biophys Acta, 1985. **828**(1): p. 13-21.
34. Schneider, C.A., W.S. Rasband, and K.W. Eliceiri, *NIH Image to ImageJ: 25 years of image analysis.* Nat Methods, 2012. **9**(7): p. 671-5.
35. Bowser, R.M., G.P. Farman, and C.C. Gregorio, *Philament: A filament tracking program to quickly and accurately analyze in vitro motility assays.* Biophys Rep (N Y), 2024. **4**(1): p. 100147.